九州大学大学院総合理工学府報告
第 37 巻 第 2 号 6-11 頁 平成 28 年 2 月

Engineering Sciences Reports, Kyushu University
Vol. 37, No. 2, pp. 6- 11, FEB, 2016

Measurement of Electron Density and Electron Temperature in Decaying Arcs Containing Decomposed Gas from Polymer

Hassaballa SAFWAT *1 and Kentaro TOMITA *2,†
†E-mail of corresponding author: tomita@ence.kyushu-u.ac.jp

(Received January 14, 2016, accepted January 22, 2016)

Electron density (n_e) and electron temperature (T_e) in arc discharges generated in the atmospheric air were measured using the laser Thomson scattering (LTS) technique. The arcs were generated using tungsten electrodes with a gap length of 2 mm. At the tip of the cathode electrode, a polymer material—polyoxymethylene (POM) or polytetrafluoroethylene (PTFE)—was inserted to generate the arcs containing the decomposed gas from polymer. LTS results showed that n_e in the arcs varied with the polymer material used. In particular, with POM, the decay speed of n_e was much higher than that with PTFE. The LTS results are qualitatively consistent with the results of previous numerical studies, which indicate that a POM ablation gas can decay the arc conductance more effectively than a PTFE ablation gas.

Key words: *Thomson scattering, Electron density, Arc discharges, Polymer, Gas circuit breaker*

1. Introduction

SF_6 gas is generally used in electric circuit breakers. However, because the global warming potential of SF_6 gas is 22,800 times higher than that of CO_2, studies on alternative gases are being conducted [1–4]. In order to conduct research to find alternative gases, understanding the characteristics of SF_6 arcs is a prerequisite. In particular, the electron density (n_e) of the arcs is one of the most important parameters because n_e is directly related with arc conductance. Therefore, we have measured n_e in decaying SF_6 gas arcs by using laser Thomson scattering (LTS) [5, 6].

Understanding of arcs containing metallic vapor or decomposed gas from polymer is also important. This is because in gas circuit breakers (GCBs), they unavoidably mix in the arcs and dramatically change the arc characteristics [7]. Therefore, several theoretical and experimental studies regarding the effect of polymers or metallic vapor on arc discharge have been performed [8–10]. However, there have been few experimental results showing the effect of the decomposed gas from polymer on n_e of the arcs.

In this study, arcs were generated with simple tungsten electrodes. In addition, at the tip of the cathode electrode, a polymer material—polyoxymethylene (POM) or polytetrafluoroethylene (PTFE)—was inserted to investigate the behavior of arcs containing decomposed gas from polymer. The results of LTS measurements showed that the spatial distribution of n_e and T_e varied with the polymer material used.

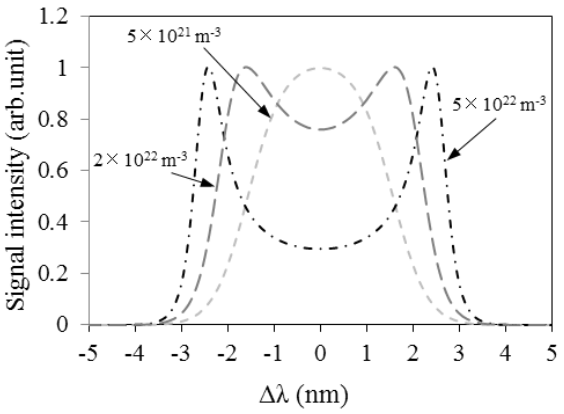

Fig.1 Theoretical curves of the Thomson scattering electron feature spectrum with n_e of 5×10^{21}, 2×10^{22}, and 5×10^{22} m^{-3}. T_e was fixed at 1eV.

*1 Department of Applied Science for Electronics and Materials, Graduate student (Present address: Physics Department, Faculty of Science, Al-Azhar University, Cairo, Egypt)
*2 Department of Electrical and Material Science

2. Method

In this study, the LTS technique was used to measure n_e and T_e of the arc discharges. Because the principle of LTS has been explained in detail previously [11, 12], only a short explanation is provided here. In addition, for convenience, we show several examples of LTS spectra obtained in this research.

Thomson scattering can be categorized by the parameter $\alpha = (k\lambda_D)^{-1}$, where k is the absolute value of the differential wavenumber vector determined by the incident-laser wavenumber vector and the scattered-light wavenumber vector, and λ_D is the Debye length of plasma. In this study, almost all spectra were in the collective regime, because α was between 0.5 and 2 [13]. In the collective regime, Thomson scattering consists of two parts: an ion feature and an electron feature. Because the spectral width of the ion feature is too narrow (<0.1 nm) to be measured with a conventional spectrometer [14, 15], only the electron feature was detected in this study. In the range of α from 0.5 to 2, n_e and T_e were estimated by the peak wavelength and the spectral shape of the electron feature [13]. Figure 1 shows the spectra predicted under the experimental condition in this study. The second harmonic of a Nd:YAG laser (λ = 532 nm) was used as a light source and scattered light at an angle of 90° from the laser path was detected.

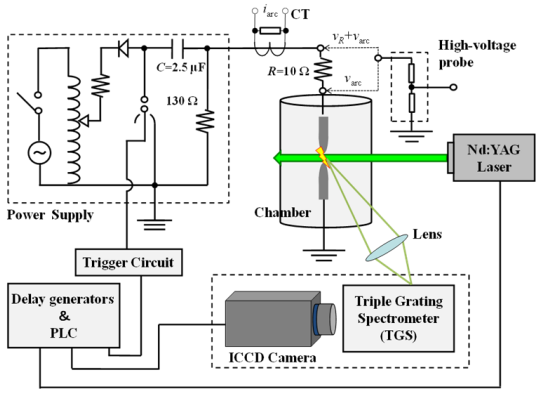

Fig.2 Arc generation and LTS system.

3. Experimental Setup

Figure 2 shows the schematic of the arc generation system and LTS system. For generating the arc discharge, a condenser with a capacitance of 2.5 μF was charged at a voltage of 7 kV. A 10 Ω resistance was added in series with the tungsten electrode. The LTS system has been calibrated using Rayleigh scattering signals from a few hundred torr of nitrogen. For LTS measurements, the second harmonic of the Nd:YAG laser (λ = 532 nm, 10 ns full width at half maximum) was used as the probing laser. The scattered light at an angle of 90° from the laser injection was collected with lenses and focused onto the entrance slit of a triple grating spectrometer (TGS). An intensified CCD camera (Princeton Instruments, PI-MAX UNIGENII) was used as the detector. The TGS was used to eliminate stray light (mainly the scattered laser light from the electrode surface) efficiently. Because the configuration of the TGS used was almost the same as that described in a previous report [16], here we only describe it briefly. The TGS consisted mainly of three diffraction gratings with 2400 lines/mm, six lenses with a focal length of 250 mm, a laser wavelength stop (0.5 mm width) to remove the stray light, an intermediate slit (0.5 mm width), and the ICCD camera. The entrance slit of the TGS was set to be 0.2 mm and the total spectral resolution was 0.3 nm. The timings of the arc generation, laser injection, and gate opening of the ICCD camera were well-synchronized with each other by using a delay pulse generator and a programmable logic controller. Figure 3 shows the schematic of the electrode setup. Both electrodes were axially symmetric and the gap length was 2 mm. The diameters of the anode and cathode were 1 mm and 10 mm, respectively. At the tip of the cathode, a polymer material, POM or PTFE, with 1 mm diameter was inserted as shown in this figure. The material of the electrode was tungsten.

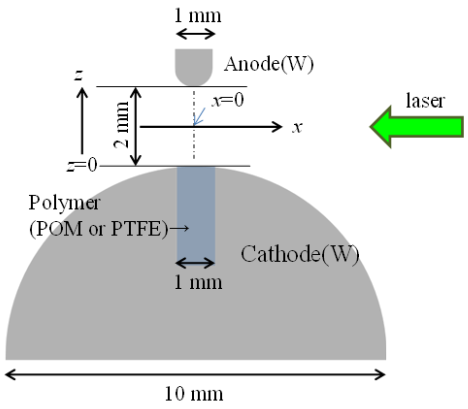

Fig.3 Schematic of the electrode setup.

4. Results

4.1. Voltage and Current Waveforms

Figure 4 shows the arc voltage waveforms, which were measured by generating the arcs with POM and PTFE. In both cases, the decay constant was 25 μs. The current waveforms were also measured. As with the voltage waveforms, the shape of the two current waveforms was the same, and the decay constant was 25 μs. The peak voltage and current were 7 kV and 700 A, respectively.

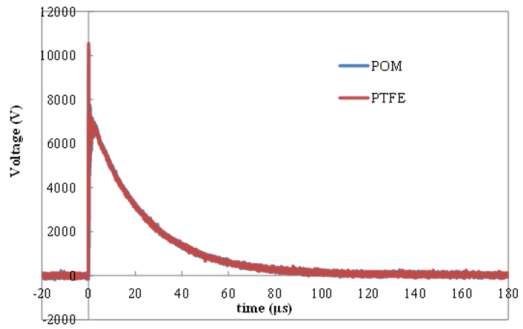

Fig.4 Arc voltage waveforms.

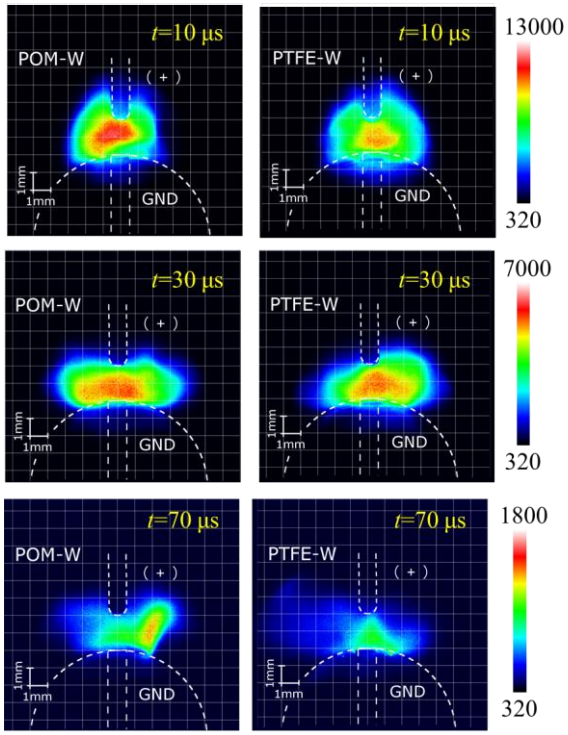

Fig.5 Self-emission of the arcs with POM and PTFE at t = 10, 30, and 70 μs.

4.2. Self-emission Measurements

Figure 5 shows the self-emission measurements of the arcs generated with the POM or PTFE polymer by using the ICCD camera. The gate width was set to 100 ns. The timings of the measurements were 10, 30, 50, 70, and 100 μs after the start of the discharge. In these figures, the emission intensity was artificially colored.

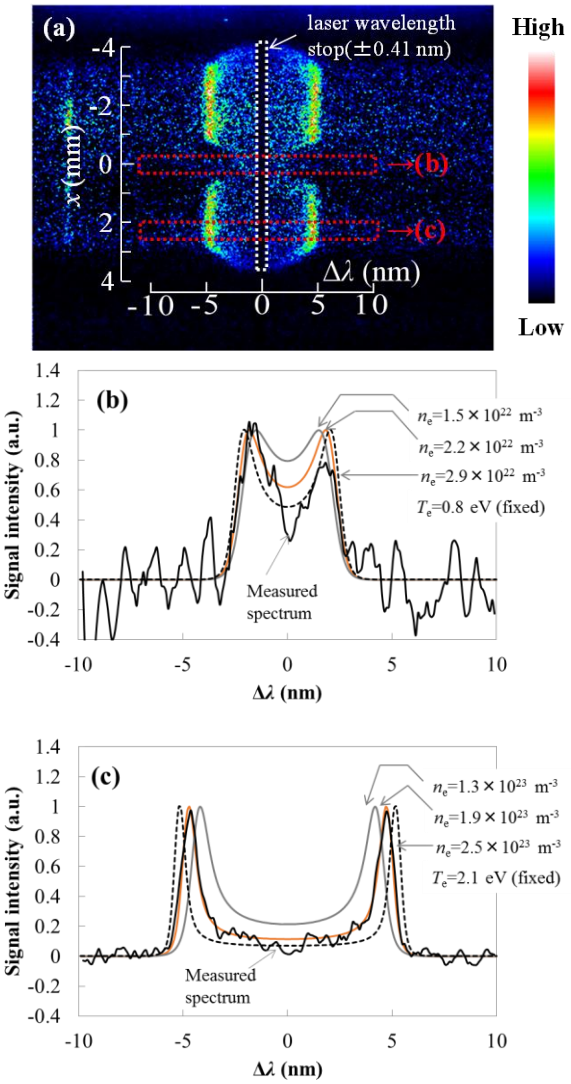

Fig.6 (a) Electron feature spectrum of the arc with POM measured at t = 10 μs and at z = 0.3 mm. (b) Spectrum extracted with x ranging from −0.3 to 0.3 mm of Fig. 6 (a). (c) Spectrum extracted with x ranging from 2.0 to 2.6 mm of Fig. 6 (a).

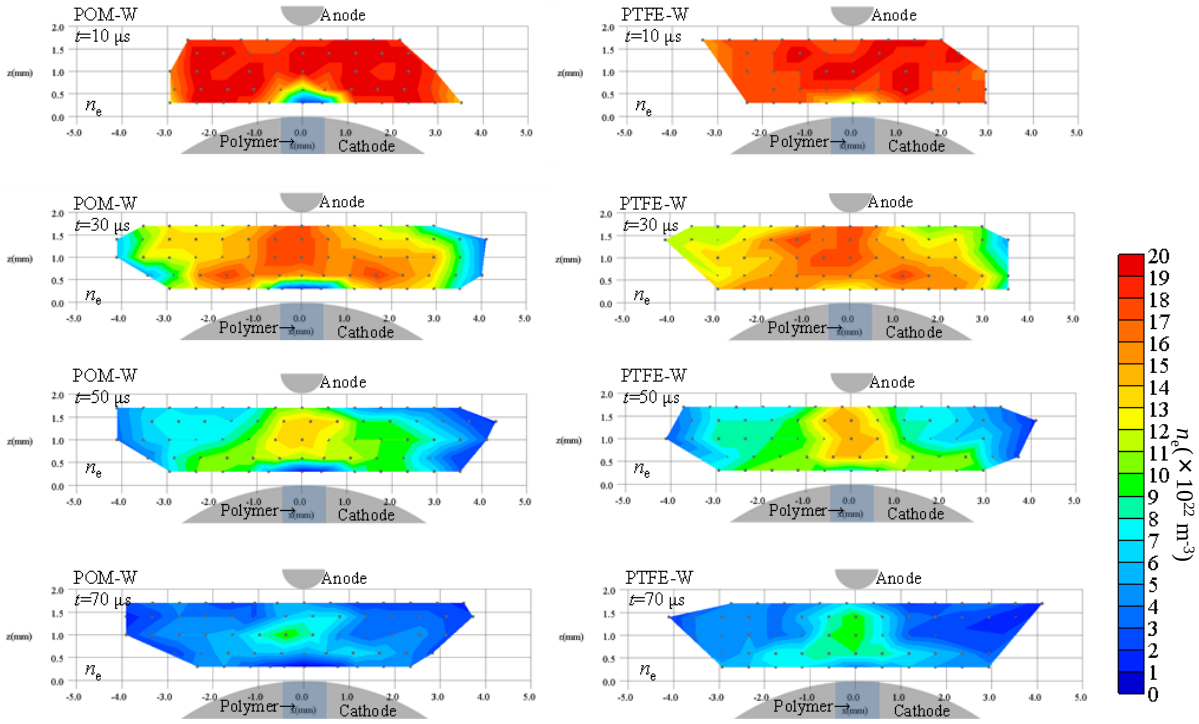

Fig.7　Spatial profiles of n_e with POM and PTFE measured at t=10, 30, 50, and 70 μs.

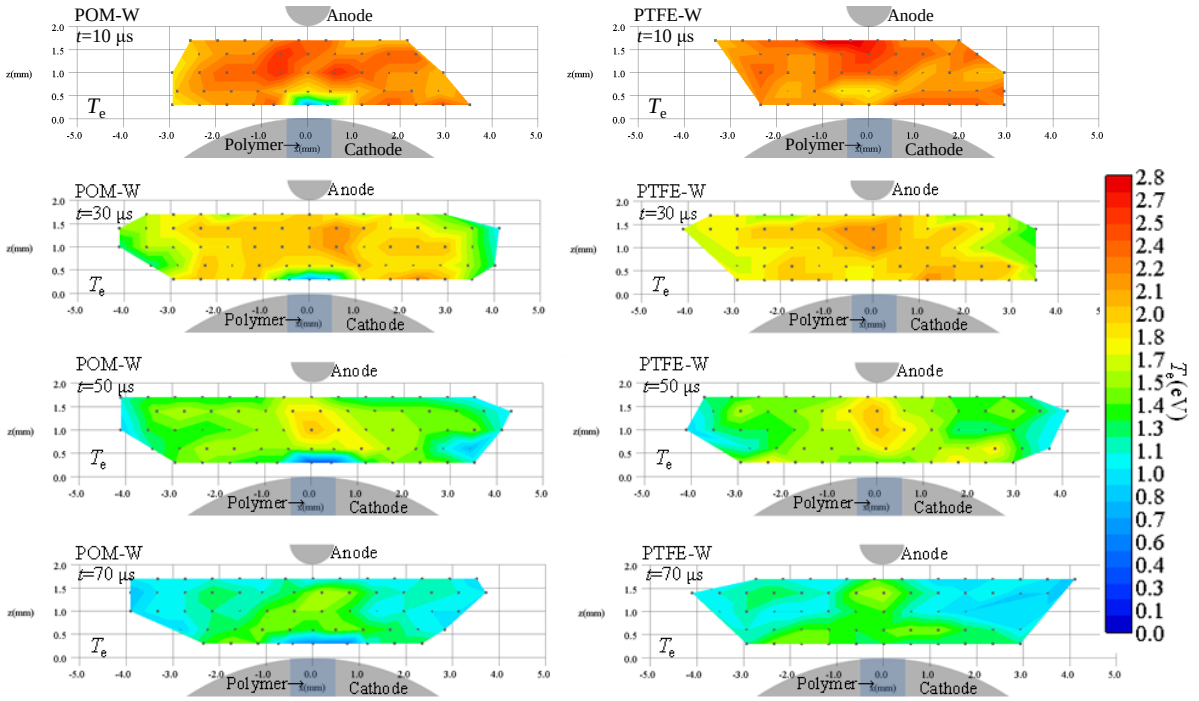

Fig.8　Spatial profiles of T_e with POM and PTFE measured at t = 10, 30, 50, and 70 μs.

4.3. Laser Thomson Scattering

Figure 6 (a) shows an example of the LTS image obtained in this study. Because an ICCD camera with 1024×1024 pixels was used as the detector in this study, the spectral information and the spatial distribution of the LTS were obtained simultaneously. Figure 6 (b) and (c) show LTS spectra extracted with x ranging from −0.3 to 0.3 mm and 2.0 to 2.6 mm, from the spectrum shown in Fig. 6 (a), respectively. The electron feature of collective Thomson scattering spectra was observed at these positions. Using theoretical fitting curves plotted in Fig. 6 (b) and (c), n_e and T_e were determined simultaneously. The LTS measurements were performed at z = 0.3, 0.6, 1.0, 1.4, and 1.7 mm and t = 10, 20, 30, 40, 50, 60, and 70 μs. At all the positions and times, n_e and T_e were determined in the same way as described previously. Figure 7 and 8 show the two-dimensional spatial profiles and temporal evolutions of n_e and T_e plotted as contour graphs. Figure 9 shows the temporal evolution of n_e and T_e at x = 0.

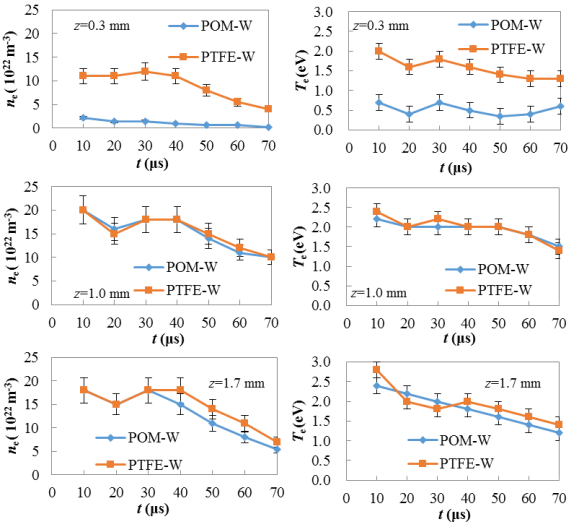

Fig.9 Temporal evolutions of n_e and T_e at z = 0.3, 1.0, and 1.7 mm (x is fixed to 0).

5. Discussion

The measurements of voltage and current waveforms show that the characteristics of the arc current and the arc voltage were almost the same even when the arcs were generated with different polymers. The decay constants of the voltage and current were both equal to 25 μs. The results indicate that their decay constants were determined from the resistance (10 Ω) and capacitance (2.5 μF) of the electrode circuit.

From the self-emission measurements, it is confirmed that the emission intensity gradually decreased after the arcs were produced. With time, the spatial distribution of the self-emission became asymmetric. However, clear differences were not observed when the different polymers were used.

Here, we discuss the results of the LTS measurements. As shown in Fig. 6 (a), the shape of the LTS spectra measured in this study has a dip around x = 0. Such a dip in collective Thomson scattering means that n_e and T_e were low at around x = 0. In our previous research, which was performed without a polymer material, the LTS spectra did not show such a dip [17]. Therefore, it seems that this spatial profile of LTS spectra is due to the influence of polymer ablation.

We estimated the region where the polymer material expanded from the cathode surface by measuring the change in the length of the polymer material. After producing arcs 200 times, the lengths of both the POM and PTFE decreased by approximately 0.2 mm. This means that 0.001 mm of POM and PTFE was ablated by the arc production on an average. The mass flux Γ_{abl} of the ablated polymer was calculated by the formula shown below:

$$\Gamma_{abl} = \frac{\rho_{pol}\Delta V_{abl}}{m_{pol}\Delta s \Delta t} \qquad (1),$$

where ρ_{pol} is the mass density in the solid state of the polymer material, ΔV_{abl} is the change in the volume of the polymer material, Δs is the surface area of the polymer material, and Δt is the time scale for polymer ablation. ρ_{pol} of POM and PTFE are 1.41×10^3 and 2.20×10^3 kg/m^3, respectively [18]. From the experimental results, $((\Delta V_{abl})/(\Delta s)) = 0.001$ mm. We assumed that Δt = 50 μs and that Γ_{abl} was constant in this time scale. The flow velocity v_{abl} was calculated as follows:

$$v_{abl} = \frac{\Gamma_{abl} m_{pol}}{\rho} \qquad (2),$$

where ρ is the mass density of the gas phase of the polymer materials. The value of ρ depends on the gas temperature. From the results of LTS measurements, gas temperatures on the surface of the polymer material were estimated as 0.3 eV for POM

and 0.7 eV for PTFE, respectively. Under these conditions, ρ = 5×10^{-2} kg/m^3 for POM and 3×10^{-2} kg/m^3 for PTFE. Accordingly, v_{abl} was calculated to be 3×10^2 m/s for POM and 1.5×10^3 m/s for PTFE. Although the method of estimation of v_{abl} is quite crude, the calculated result implies that the ablated polymer expands to the region where the LTS was performed.

As can be seen from Figure 7 and Figure 8, near the cathode region, n_e of the arc with POM was smaller than that with PTFE. In particular, at z = 0.3 mm, n_e of the arc with POM was approximately 10 times smaller than that with PTFE.

In Ref. [18], the conductance of arcs containing POM and PTFE has been investigated by numerical calculations. The results show that POM can decay the arc conductance more effectively than PTFE. It is noted that this difference is caused by the thermal conductivity and electrical conductivity of POM and PTFE. The LTS results are qualitatively consistent with the results of the numerical analysis and the thermal and electrical properties of POM and PTFE.

6. Conclusion

This paper presented the experimental approach to understand the characteristics of arcs containing decomposed gas from polymer. POM and PTFE were used as the polymer materials. The measurements of voltage, current, and self-emission did not show any clear differences when the polymer used as the ablation gas was changed. On the contrary, the LTS results clearly showed that n_e and T_e changed in the arcs with different polymers because of ablation. These results indicate that Thomson scattering can be a powerful method to study arcs containing decomposed gas from polymer.

Acknowledgments

The authors wish to thank Professor Kiichiro Uchino and Mr. Daisuke Gojima from the Interdisciplinary Graduate School of Engineering Sciences, Kyushu University for their substantial support of the study.

References

1) L. G. Christophorou et al., NIST Technical Note 1425 (1997).
2) S.A. Boggs et al., Gas-Insulated Substations (New York: Pergamon Press) (1986).
3) W. T. Shugg et al., Handbook of Electrical and Electronic Insulating Materials, Second Edition (New York: IEEE Press) (1995).
4) L. G. Christophorou et al., IEEE Trans. Dielectr. Electr. Insul. 2, 952 (1995).
5) K. Tomita et al., J. Phys. D. Appl. Phys. 48, 265201 (2015).
6) K. Tomita et al., J. Phys. D. Appl. Phys. 46, 382001 (2013).
7) P. Teulet et al., J. Phys. D. Appl. Phys. 42, 175201 (2009).
8) A. Gleizes, et al., J. Phys. D. Appl. Phys. 38, R153 (2005).
9) T. Sakuda et al., IEEJ Trans. FM 98, 209 (1978) (in Japanese).
10) H. Ohno et al., IEEJ Trans. PE 108, 157 (1988) (in Japanese).
11) D. H. Froula et al., Plasma Scattering of Electromagnetic Radiation, Second Edition (New York: Academic) (2011).
12) D. E. Evans et al., Rep. Prog. Phys. 32, 207 (1969).
13) K. Tomita et al., J. Inst. 7, C02057 (2012).
14) K. Tomita et al., Appl. Phys. Express 8, 126101 (2015).
15) K. Tomita et al., Appl. Phys. Express 6, 076101 (2013).
16) S. Hasaballa et al., IEEE Trans. Plasma Sci. 32, 127 (2004).
17) K. Tomita et al., Electrical Engineering in Japan 188, 1 (2014) (Translated from Denki Gakkai Ronbunshi, Vol. 133-A, No. 9, September 2013, pp. 458–464).
18) T. Onchi et al., IEEJ Trans. PE, 131, 609 (2011) (in Japanese).